

Coaction and competition between the ferroelectric field effect and the strain effect in $\text{Pr}_{0.5}\text{Ca}_{0.5}\text{MnO}_3$ film/ $0.67\text{Pb}(\text{Mg}_{1/3}\text{Nb}_{2/3})\text{O}_3$ - 0.33PbTiO_3 crystal heterostructures

Q. X. Zhu, W. Wang, S. W. Yang, X. M. Li, Y. Wang et al.

Citation: *Appl. Phys. Lett.* **101**, 172906 (2012); doi: 10.1063/1.4761948

View online: <http://dx.doi.org/10.1063/1.4761948>

View Table of Contents: <http://apl.aip.org/resource/1/APPLAB/v101/i17>

Published by the American Institute of Physics.

Related Articles

Structural and electrical properties of atomic layer deposited Al-doped ZrO_2 films and of the interface with TaN electrode

J. Appl. Phys. **112**, 014107 (2012)

Tunnel electroresistance in junctions with ultrathin ferroelectric $\text{Pb}(\text{Zr}_{0.2}\text{Ti}_{0.8})\text{O}_3$ barriers

Appl. Phys. Lett. **100**, 232902 (2012)

Polarization and interface charge coupling in ferroelectric/ $\text{AlGaIn}/\text{GaIn}$ heterostructure

Appl. Phys. Lett. **100**, 112902 (2012)

Ultrahigh dielectric constant of thin films obtained by electrostatic force microscopy and artificial neural networks

Appl. Phys. Lett. **100**, 023101 (2012)

Converse-piezoelectric effect on current-voltage characteristics of symmetric ferroelectric tunnel junctions

J. Appl. Phys. **111**, 014103 (2012)

Additional information on *Appl. Phys. Lett.*

Journal Homepage: <http://apl.aip.org/>

Journal Information: http://apl.aip.org/about/about_the_journal

Top downloads: http://apl.aip.org/features/most_downloaded

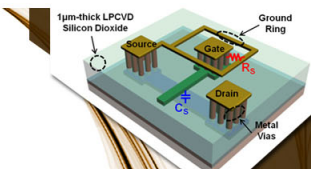
Information for Authors: <http://apl.aip.org/authors>

ADVERTISEMENT

AIP | Applied Physics
Letters


**EXPLORE WHAT'S
NEW IN APL**

SUBMIT YOUR PAPER NOW!



**SURFACES AND
INTERFACES**

Focusing on physical, chemical, biological, structural, optical, magnetic and electrical properties of surfaces and interfaces, and more...



**ENERGY CONVERSION
AND STORAGE**

Focusing on all aspects of static and dynamic energy conversion, energy storage, photovoltaics, solar fuels, batteries, capacitors, thermoelectrics, and more...

Coaction and competition between the ferroelectric field effect and the strain effect in $\text{Pr}_{0.5}\text{Ca}_{0.5}\text{MnO}_3$ film/ $0.67\text{Pb}(\text{Mg}_{1/3}\text{Nb}_{2/3})\text{O}_3$ - 0.33PbTiO_3 crystal heterostructures

Q. X. Zhu,¹ W. Wang,¹ S. W. Yang,² X. M. Li,^{1,a)} Y. Wang,³ H.-U. Habermeier,⁴ H. S. Luo,¹ H. L. W. Chan,³ X. G. Li,² and R. K. Zheng^{1,b)}

¹State Key Laboratory of High Performance Ceramics and Superfine Microstructure, Shanghai Institute of Ceramics, Chinese Academy of Sciences, Shanghai 200050, China

²Hefei National Laboratory for Physical Sciences at Microscale and Department of Physics, University of Science and Technology of China, Hefei 230026, China

³Department of Applied Physics and Materials Research Center, The Hong Kong Polytechnic University, Hong Kong

⁴Max Planck Institute for Solid State Research, Heisenbergstrasse 1, D-70569 Stuttgart, Germany

(Received 26 June 2012; accepted 8 October 2012; published online 24 October 2012)

The coaction and competition between the ferroelectric field effect and the strain effect in $\text{Pr}_{0.5}\text{Ca}_{0.5}\text{MnO}_3$ (PCMO) film/ $0.67\text{Pb}(\text{Mg}_{1/3}\text{Nb}_{2/3})\text{O}_3$ - 0.33PbTiO_3 crystal heterostructures were studied. Based on different types of resistance-electric field hysteresis loops at various temperatures, it is clearly identified that the strain effect dominates over the ferroelectric field effect for temperature T above the charge-ordering temperature T_{CO} of PCMO. With the strong localization of charge carriers for $T < T_{\text{CO}}$, the ferroelectric field effect strongly competes with the strain effect and finally dominates over the latter for $T < 0.8T_{\text{CO}}$. Moreover, the poling-induced strain effect is considerably enhanced by a magnetic field, demonstrating the important role of the phase separation in understanding the strain effect in such heterostructures. © 2012 American Institute of Physics. [<http://dx.doi.org/10.1063/1.4761948>]

The electric-field control of electronic and magnetic properties of complex oxide thin films epitaxially grown on ferroelectric (FE) single-crystal substrates has attracted much attention due to their rich physics and potential applications in multifunctional devices.^{1–9} There are a number of reports on this topic for perovskite manganite film/FE crystal heterostructures, such as $\text{La}_{0.67}\text{Sr}_{0.33}\text{MnO}_3$ film/ BaTiO_3 crystal³ and $\text{La}_{1-x}\text{A}_x\text{MnO}_3$ ($\text{A} = \text{Ca}, \text{Sr}, \text{Ba}$) film/ $(1-x)\text{Pb}(\text{Mg}_{1/3}\text{Nb}_{2/3})\text{O}_3$ - $x\text{PbTiO}_3$ crystal^{4–9} heterostructures. It is generally believed that the electric-field-controlled tunability of electronic and magnetic properties of manganite thin films is *strain-induced* for such heterostructures.^{3–9} However, one has to be reminded that the FE single-crystal substrate is a ferroelectric material, the manganite film/FE crystal heterostructure can be viewed as a ferroelectric field effect transistor where the manganite film and the FE substrate are the conductive channel and the insulating gate, respectively. If a gate voltage is applied to the FE substrate, the charge carrier density of the manganite thin film would be modified due to the accumulation or depletion of charge carriers at interface, arising from the ferroelectric field effect.^{10,11} Due to the strong interplay among spin, charge, lattice, and orbital degrees of freedom,^{12,13} the properties of manganite films are particularly sensitive to the charge carrier concentration. Unfortunately, there have been few reports about the ferroelectric field effect on the electronic transport properties in such heterostructures so far. $\text{Pr}_{0.5}\text{Ca}_{0.5}\text{MnO}_3$ (PCMO) is an interesting spin, charge, and orbital-ordered manganite with the coexistence of ferromagnetic and charge-ordered

antiferromagnetic phases at low temperatures under external perturbations such as magnetic field,¹⁴ electric field,¹⁵ or electromagnetic radiation.¹⁶ While $0.67\text{Pb}(\text{Mg}_{1/3}\text{Nb}_{2/3})\text{O}_3$ - 0.33PbTiO_3 (PMN-PT) single crystal is a ferroelectric material with coexistence of monoclinic, rhombohedral, and tetragonal phases at room temperature, and thus displays extraordinary ferroelectric and piezoelectric activities¹⁷ and can be used as ferroelectric substrate to grow perovskite manganite thin films.^{4–9,18}

In this letter, we fabricate PCMO film/PMN-PT crystal heterostructures and demonstrate that the ferroelectric field effect has a dramatic impact on the electronic transport properties of the PCMO film. Although the electric-field-induced strain in the PMN-PT substrate can be transferred to the epitaxial PCMO film continuously and reversibly, our results give strong evidence that the coaction and competition between the ferroelectric field effect and the strain effect exist in PCMO film/PMN-PT crystal heterostructures. The interaction between the strain effect and ferroelectric field effect leads to a remarkable temperature dependent electric-field-manipulation of the electronic transport behavior.

PCMO films were deposited on one-side-polished and (001)-oriented PMN-PT single-crystal substrates using dc magnetron sputtering.¹⁹ The thickness of films was measured to be ~ 32 nm using a JSM-6700 F scanning electron microscope. The surface morphology of films was obtained using an atomic force microscope (Nanocute SII, Seiko, Japan). The phase purity and epitaxial relationship of the heterostructure were investigated by x-ray diffraction (XRD) θ - 2θ scan and ϕ -scan, respectively, using a Bruker D8 Discover x-ray diffractometer. Magnetotransport properties of PCMO films between the two top-top gold electrodes (see the lower

^{a)}Electronic mail: lixm@mail.sic.ac.cn.

^{b)}Electronic mail: zrk@ustc.edu.

inset of Fig. 2) were measured using a physical property measurement system (PPMS-9, Quantum Design). The two top-top gold electrodes were prepared by magnetron sputtering in order to form ohmic contact between the gold electrodes and the PCMO film. The contact resistance (less than several ohms) is much smaller than that of the PCMO film ($\sim 13 \text{ k}\Omega$ at room temperature), and thus, is neglected here. External electric field was applied to the PMN-PT substrate through the top and bottom gold electrodes. A laser interferometer (SIOS NT-04 Sensor) was employed to analyze the strain versus electric field hysteresis loop of the PMN-PT substrate at $T = 296 \text{ K}$.

Fig. 1(a) shows the XRD θ - 2θ scan for the PCMO/PMN-PT heterostructure, demonstrating that the PCMO film is highly c -axis preferentially oriented and without any impurity phases. Despite a relatively large lattice mismatch between the PMN-PT (4.02 \AA) and the PCMO, the film still grows epitaxially on the PMN-PT crystal, as illustrated from the Φ -scan patterns of PCMO (101) and PMN-PT (101) planes [Fig. 1(b)]. The PMN-PT substrate exhibits excellent piezoelectric properties, which is evidenced by a well-defined butterflylike strain-electric field hysteresis loop [Fig. 1(c)]. Fig. 1(d) is the surface morphology of the PCMO film with a root-mean-square roughness of $\sim 1.2 \text{ nm}$.

To probe the strain effect and the ferroelectric field effect in the PCMO/PMN-PT structure, the relative change in the resistance $\Delta R/R$ [$\Delta R/R = [R(E) - R(0)]/R(0)$] of the PCMO film between the two top-top gold electrodes was measured as a function of the electric field E applied to the PMN-PT substrate at $T = 296 \text{ K}$ employing the electrical measurement circuit shown in the lower inset of Fig. 2. Initially, the PMN-PT substrate was in the unpoled state (denoted by P_r^0). During the poling of the PMN-PT substrate,

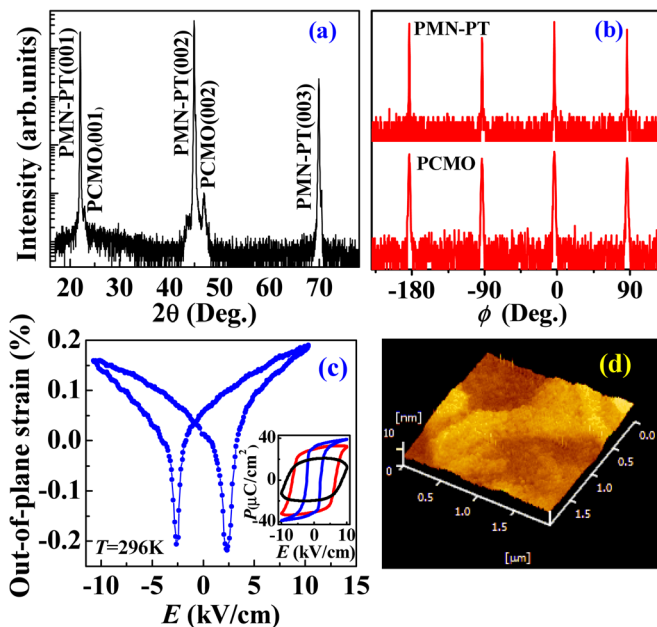


FIG. 1. (a) X-ray diffraction pattern for the PCMO/PMN-PT structure. (b) XRD ϕ scans taken on the PCMO (101) and PMN-PT (101) diffraction peaks, respectively. (c) Out-of-plane piezo-strain versus E for the PMN-PT substrate at 296 K . The inset is the P - E hysteresis loop for the PMN-PT substrate at 296 K (the blue one), 180 K (the red one), and 150 K (the black one), respectively. (d) The surface morphology of the PCMO film.

the resistance of the PCMO film was measured simultaneously. Note that the direction of the polarization points toward the PCMO film (denoted by P_r^+), as schematically shown in the lower inset of Fig. 2. The resistance is nearly field-independent for $E \leq 2 \text{ kV/cm}$ but decreases considerably in the field region of $2 \text{ kV/cm} < E < 3 \text{ kV/cm}$. For $E > 4 \text{ kV/cm}$, the resistance decreases linearly with increasing E , which is a typical behavior of the resistance due to the converse piezoelectric effect of the PMN-PT substrate.^{19,20} The large decrease in the resistance near the coercive field E_C of the PMN-PT substrate is similar to that observed in the $\text{LaMnO}_{3+\delta}$ /PMN-PT structure²¹ where the strain state of the $\text{LaMnO}_{3+\delta}$ film was modified by the poling-induced strain in the PMN-PT substrate. *In situ* XRD θ - 2θ scan performed near the PMN-PT(002) and PCMO(002) diffraction peaks shows that the lattice constants c of the PMN-PT substrate and the PCMO film for $E = 10 \text{ kV/cm}$ are indeed larger than those for $E = 0 \text{ kV/cm}$, reflected by the shift of the diffraction peaks towards lower 2θ angles (see the upper inset of Fig. 2). Furthermore, the PMN-PT(020)/(200) diffraction peaks on the right hand side of PMN-PT(002) diffraction peak disappear when $E = 10 \text{ kV/cm}$ was applied to the PMN-PT substrate, which indicates that the in-plane a - or b -axis oriented ferroelectric domains rotate towards the electric-field direction (i.e., c -axis). It should be highlighted that the electric field not only induces strain via the rotation of polarization direction but also induces electric charges at interface between the PCMO film and the PMN-PT crystal (i.e., the ferroelectric field effect). If the ferroelectric field effect is taken into account, the depletion of holes will happen in the PCMO film^{10,11} within screen length when applying positive electric field to the PMN-PT substrate, thereby leading to an increase in the resistance. Nevertheless, the actual sign of the change in the resistance is opposite to that expected from the ferroelectric field effect (see Fig. 2). Since the applied electric field will be screened within several unit cells in the film and could not affect bulk transport properties of the film,²² it is thus believed that the electric-field induced decrease in the resistance at $T = 296 \text{ K}$ is mainly strain-induced. As a general tendency, the in-plane tensile strain tends to stabilize the

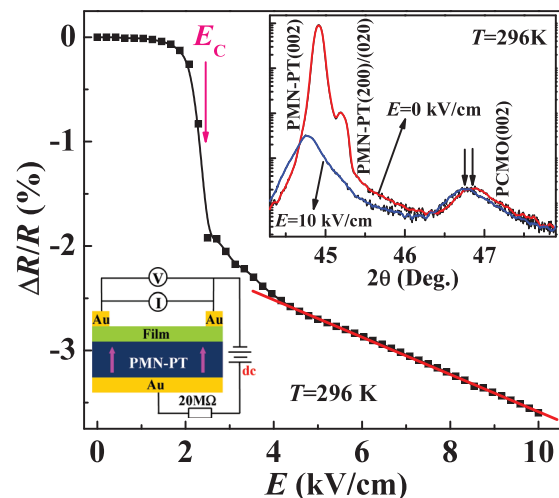


FIG. 2. Relative change in the resistance of the PCMO film as a function of E applied to the PCMO/PMN-PT structure. The upper inset shows the XRD patterns in the vicinity of (002) diffraction peaks under $E = 0$ and 10 kV/cm .

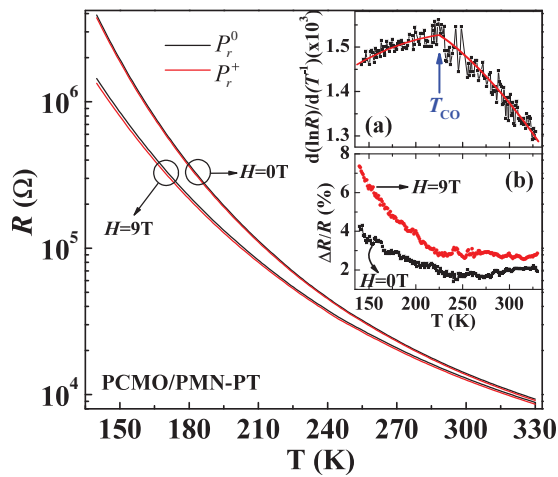


FIG. 3. Temperature dependence of the resistance for the PCMO film at $H=0$ and 9 T when the PMN-PT substrate was in the P_r^0 and P_r^+ states, respectively. The upper panel of the inset shows the $d(\ln R)/d(T^{-1})$ - T curve for the PCMO film. The lower panel shows strain-induced $\Delta R/R$ for the PCMO film under $H=0$ and 9 T, respectively.

charge-ordered insulating phase for manganite thin films.^{23,24} The electric-field-induced large drop in the resistance near E_C could be due to the partial release of tensile strain resulted from poling-induced strain in the PMN-PT substrate.²¹

Figure 3 presents how the resistance (R) of the PCMO film evolves as a function of temperature (T) in zero magnetic field ($H=0$ T) and a magnetic field of $H=9$ T when the PMN-PT substrate was in the unpoled and positively poled state, respectively. Note that after the PMN-PT substrate had been poled to the P_r^+ state, the poling field was turned off. Since the ferroelectric Curie temperature of the PMN-PT substrate is 430 K, much higher than 330 K (i.e., the highest temperature in the R - T curve), the polarization direction would remain toward the field direction in the whole temperature range, that is, at low temperatures the effect of poling-induced remnant strain on the resistance is the same as that at room temperature, which is reflected by the fact that the resistance at any fixed temperature for P_r^+ is smaller than that for P_r^0 (see Fig. 3). It is known that the R - T curve for charge-ordered manganites can be used to determine the charge-ordering transition temperature T_{CO} where the resistance shows an abrupt upturn when the temperature is lowered through T_{CO} .¹⁴ While for charge-ordered manganite films, this signature is usually weaker and less sharply defined, but T_{CO} can still be extracted by plotting $d(\ln R)/d(T^{-1})$ against T .^{19,25} The $d(\ln R)/d(T^{-1})$ - T curve shows a remarkable change in slope at $T \sim 225$ K [inset (a) of Fig. 3], implying that the charge ordering phase transition occurs near that temperature. In addition, we present the poling-strain-induced $\Delta R/R$ as a function of temperature under $H=0$ and 9 T in the inset (b) of Fig. 3. Here $\Delta R/R$ is defined as $\Delta R/R = [R(P_r^0, H) - R(P_r^+, H)]/R(P_r^0, H)$. One can see that the magnetic field of 9 T enhances the strain effect and thus brings stronger strain-tunability of the resistance of the PCMO film. At $T=140$ K, the poling-strain-induced $\Delta R/R$ is enhanced by $\sim 73\%$ [inset (b) of Fig. 3] by a magnetic field of 9 T, indicating a strong coupling between the strain effect and the magnetic field. Zheng *et al.*^{7,9} recently reported a

strong correlation between the strain and the phase separation for manganite thin films, i.e., the stronger the phase separation, the larger the strain-induced change in the resistance. The magnetic-field-induced large decrease in the resistance (see Fig. 3) indicates that a high magnetic field of 9 T converts a considerable fraction of the charge-ordered antiferromagnetic insulating phase to the ferromagnetic metallic phase,^{14,26,27} namely, the phase separation tendency is enhanced by the magnetic field. As a result, the strain-tunability of the resistance is enhanced due to the enhanced phase separation in the PCMO film.

To further probe into the strain and ferroelectric field effects, the resistance of the PCMO film was measured as a function of bipolar electric field at various fixed temperatures (see Fig. 4). It is noted that, if the ferroelectric field effect plays a dominant role in influencing the electronic transport properties of the PCMO film, the resistance versus electric field (R - E) hysteresis loop should show a rectangular shape with the resistance change exhibiting opposite signs for opposite directions of applied electric field, as previously observed in $\text{La}_{1-x}\text{Ba}_x\text{MnO}_3$ ($x=0.1, 0.15$)/ $\text{PbZr}_{0.2}\text{Ti}_{0.8}\text{TiO}_3$ (Ref. 11) and $\text{La}_{0.8}\text{Ca}_{0.2}\text{MnO}_3/\text{Pb}((\text{Zr}_{0.2}\text{Ti}_{0.8})\text{O}_3)$ (Ref. 28) ferroelectric field effect transistors. In contrast, if the strain effect has greater influence on the electronic transport properties, the R - E hysteresis loop should show a butterflylike shape with the resistance change exhibiting the same sign for opposite directions of applied electric field, as those observed in the $\text{La}_{0.7}\text{Sr}_{0.3}\text{MnO}_3/0.72\text{Pb}(\text{Mg}_{1/3}\text{Nb}_{2/3})\text{O}_3$ - 0.28PbTiO_3 (Ref. 5) and $\text{La}_{0.7}\text{Sr}_{0.3}\text{CoO}_3/0.72\text{Pb}(\text{Mg}_{1/3}\text{Nb}_{2/3})\text{O}_3$ - 0.28PbTiO_3 (Ref. 29) systems. Fig. 4(b) shows that the R - E hysteresis loop has a roughly symmetrical butterflylike

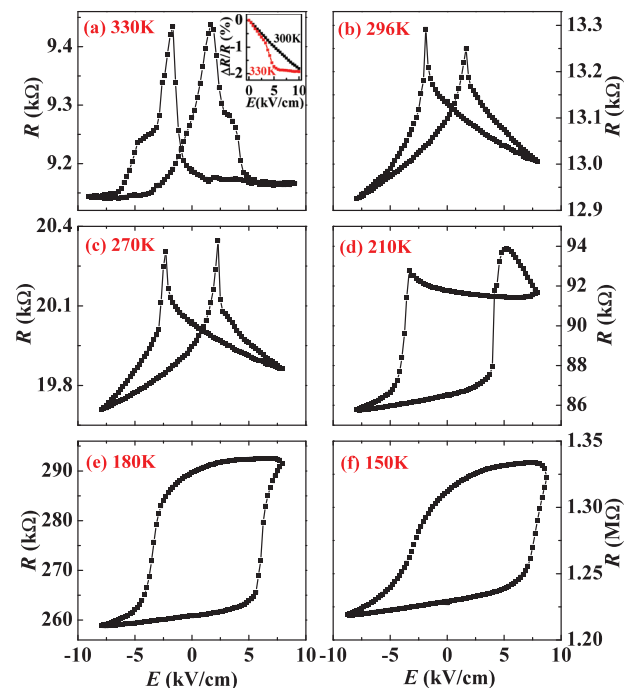


FIG. 4. Change in the resistance of the PCMO film at several fixed temperatures as a function of bipolar electric field applied to the PMN-PT substrate. The inset of (a) presents the change in the resistance of the PCMO film when positive electric field applied to positively poled PMN-PT substrate at 300 and 330 K, respectively.

shape at 296 K, which is the typical behavior of the resistance modification due to the polarization-rotation-induced strain in the PMN-PT substrate.^{5,21,29} Note that the out-of-plane strain versus E hysteresis loop for the PMN-PT substrate also show butterflylike shape at $T = 296$ K [see Fig. 1(c)], which strongly demonstrates that the butterflylike modulation of the resistance is indeed strain-induced. We thus believe that the ferroelectric field effect has a minor effect on the electronic transport properties of the PCMO film at 296 K. It is obvious that the general shape of the R - E hysteresis loop at $T = 330$ K [Fig. 4(a)] is also butterflylike, however, around $E = \pm 4$ kV/cm the curve is not smooth with sharply-changed points, resulting from an electric field-induced rhombohedral-to-tetragonal structural phase transition in the PMN-PT substrate,^{30,31} which was further evidenced by the pronounced drop of the resistance at the structural phase transition point by sweeping the electric field from 0 to 10 kV/cm at $T = 330$ K [see the inset of Fig. 4(a)]. Here, the direction of the electric field is the same as the polarization direction. The much weaker response of the resistance to the piezoelectric strain above the transition field (i.e., $E > 5$ kV/cm) reveals that the high-field phase is the tetragonal one. With decreasing temperature from 296 K, the symmetry of R - E hysteresis loop is reduced with the resistance values for negative electric field lower than those for positive electric field [see Figs. 4(c) and 4(d)], which is ascribed to that the positive polarization of the PMN-PT layer will lead to a depletion of holes in the PCMO film and thus an increase in the resistance while the negative polarization of the PMN-PT layer will cause an accumulation of holes in the PCMO film and thus a decrease in the resistance. The change of the R - E hysteresis loops from a butterflylike shape [Figs. 4(a) and 4(b)] to a rectangular-like shape [Figs. 4(d) and 4(e)] indicates that the relative importance of the ferroelectric field effect increases while that of the strain effect decreases with decreasing temperature. The former finally dominates over the latter as the temperature further decreases to a certain temperature (e.g., $T = 180$ K). The enhanced ferroelectric field effect at low temperatures ($T \leq T_{CO}$), agrees with the feature that the charge carriers gradually localize with decreasing temperature from room temperature. Particularly, below T_{CO} the charge carriers become strongly localized and ordered,^{14,15} leading to a lower concentration of mobile carriers. According to ferroelectric field effect, the lower the areal charge carrier density n , the larger the relative change in the areal charge carrier density $\Delta n/n$. In a free electron model, one could obtain the relationship that $\Delta R/R = -\Delta n/n$.^{11,32} Here, Δn can be expressed as $\Delta n = \Delta P/e$ ¹¹ where Δn , ΔP , and e are the electrostatic-field-induced change in the areal charge carrier density, the remnant polarization of the PMN-PT substrate, and the unit charge (1.6×10^{-19} C), respectively.

With further decreasing temperature from 180 K, the rectangular-like R - E loop starts shrinking and becomes slim [see Fig. 4(f)]. We stress that similar behaviors for the polarization-electric field (P - E) loop were observed for the PMN-PT substrate³³ [also see the inset of Fig. 1(c)], where the coercive field is so large at low temperature that a voltage of 480 V (i.e., 10 kV/cm) is apparently inadequate to align ferroelectric domains towards the field direction, leading to

the gradual collapse of the P - E loop. The similarity in the shape and coercive field between the P - E loop and the R - E loop gives another evidence that at low temperatures the resistance change in the PCMO channel is attributed to the ferroelectric field effect at interface.

In summary, based on different types of R - E hysteresis loops at various temperatures, we identified that the ferroelectric field effect is minor for $T > T_{CO}$ in the PCMO/PMN-PT structure. However, for $T < T_{CO}$, due to the charge ordering, the ferroelectric field effect plays a more and more important role and competes with the strain effect and totally dominates over the strain effect at lower temperatures. Furthermore, the magnetic field considerably enhances the strain-tunability of the resistance for the PCMO film, implying that the strain effect are closely related to the phase separation which is crucial to understand the interfacial strain effect in manganite film/ferroelectric crystal heterostructures. The clear identification of the crucial role of the ferroelectric field effect would be important not only for understanding the profound physics in manganite/FE heterostructures, but also for their potential application in functional devices.

This work was supported by the NSFC (Grant Nos. 51172259, 50832007, and 11090332), the 973 Program (Grant Nos. 2009CB623304 and 2012CB922003), the CAS/SAFEA International Partnership Program for Creative Research Teams, and the PolyU internal (Grant No. G-U846).

¹Y. Yang, Z. L. Luo, H. Huang, Y. Gao, J. Bao, X. G. Li, S. Zhang, Y. G. Zhao, X. Chen, G. Pan, and C. Gao, *Appl. Phys. Lett.* **98**, 153509 (2011).

²J. J. Yang, Y. G. Zhao, H. F. Tian, L. B. Luo, H. Y. Zhang, Y. J. He, and H. S. Luo, *Appl. Phys. Lett.* **94**, 212504 (2009).

³W. Eerenstein, M. Wiora, J. L. Prieto, J. F. Scott, and N. D. Mathur, *Nature Mater.* **6**, 348 (2007).

⁴K. Dörr, O. Bilani-Zeneli, A. Herklotz, A. D. Rata, K. Boldyreva, J. W. Kim, M. C. Dekker, K. Nenkov, L. Schultz, and M. Reibold, *Eur. Phys. J. B* **71**, 361 (2009).

⁵C. Thiele, K. Dörr, S. Fähler, L. Schultz, D. C. Meyer, A. A. Levin, and P. Paufler, *Appl. Phys. Lett.* **87**, 262502 (2005).

⁶C. Thiele, K. Dörr, O. Bilani, J. Rödel, and L. Schultz, *Phys. Rev. B* **75**, 054408 (2007).

⁷R. K. Zheng, Y. Wang, Y. K. Liu, G. Y. Gao, L. F. Fei, Y. Jiang, H. L. W. Chan, X. M. Li, H. S. Luo, and X. G. Li, *Mater. Chem. Phys.* **133**, 42 (2012).

⁸J. Wang, F. X. Hu, L. Chen, J. R. Sun, and B. G. Shen, *J. Appl. Phys.* **109**, 07D715 (2011).

⁹R. K. Zheng, Y. Jiang, Y. Wang, H. L. W. Chan, C. L. Choy, and H. S. Luo, *Phys. Rev. B* **79**, 174420 (2009).

¹⁰S. Mathews, R. Ramesh, T. Venkatesan, and J. Benedetto, *Science* **276**, 238 (1997).

¹¹T. Kanki, Y.-G. Park, H. Tanaka, and T. Kawai, *Appl. Phys. Lett.* **83**, 4860 (2003).

¹²A. K. Sarychev, S. O. Boyarintsev, A. L. Rakhmanov, K. I. Kugel, and Y. P. Sukhorukov, *Phys. Rev. Lett.* **107**, 267401 (2011).

¹³T. Z. Ward, J. D. Budai, Z. Gai, J. Z. Tischler, L. F. Yin, and J. Shen, *Nat. Phys.* **5**, 885 (2009).

¹⁴Y. Tomioka, A. Asamitsu, H. Kuwahara, and Y. Moritomo, *Phys. Rev. B* **53**, R1689 (1996).

¹⁵A. Asamitsu, Y. Tomioka, H. Kuwahara, and Y. Tokura, *Nature* **388**, 50 (1997).

¹⁶K. Ogawa, W. Wei, K. Miyano, Y. Tomioka, and Y. Tokura, *Phys. Rev. B* **57**, 15033 (1998).

¹⁷S.-E. Park and T. R. Shroud, *J. Appl. Phys.* **82**, 1804 (1997).

¹⁸E. J. Guo, J. Gao, and H. B. Lu, *Appl. Phys. Lett.* **98**, 081903 (2011).

¹⁹R. K. Zheng, C. Chao, H. L. W. Chan, C. L. Choy, and H. S. Luo, *Phys. Rev. B* **75**, 024110 (2007).

²⁰R. K. Zheng, Y. Jiang, Y. Wang, H. L. W. Chan, C. L. Choy, and H. S. Luo, *Appl. Phys. Lett.* **93**, 102904 (2008).

- ²¹R. K. Zheng, H. U. Habermeier, H. L. W. Chan, C. L. Choy, and H. S. Luo, *Phys. Rev. B* **81**, 104427 (2010).
- ²²T. Wu, S. Ogale, J. Garrison, B. Nagaraj, A. Biswas, Z. Chen, R. Greene, R. Ramesh, T. Venkatesan, and A. J. Millis, *Phys. Rev. Lett.* **86**, 5998 (2001).
- ²³D. Gillaspie, J. X. Ma, H.-Y. Zhai, T. Z. Ward, H. M. Christen, E. W. Plummer, and J. Shen, *J. Appl. Phys.* **99**, 08S901 (2006).
- ²⁴W. Prellier, E. Buzin, C. Simon, B. Mercey, M. Hervieu, S. de Brion, and G. Chouteau, *Phys. Rev. B* **66**, 024432 (2002).
- ²⁵A. P. Ramirez, P. Schiffer, S.-W. Cheong, C. H. Chen, W. Bao, T. T. M. Palstra, P. L. Gammel, D. J. Bishop, and B. Zegarski, *Phys. Rev. Lett.* **76**, 3188 (1996).
- ²⁶D. K. Baisnab, T. G. Kumary, A. T. Satya, A. Mani, J. Janaki, R. Nithya, L. S. Vaidhyanathan, M. P. Janawadkar, and A. Bharathi, *J. Magn. Magn. Mater.* **323**, 2823 (2011).
- ²⁷A. Karmakar, S. Majumdar, A. K. Singh, S. Patnaik, and S. Giri, *J. Magn. Magn. Mater.* **324**, 649 (2012).
- ²⁸T. Zhao, S. B. Ogale, S. R. Shinde, R. Ramesh, R. Droopad, J. Yu, K. Eisenbeiser, and J. Misewich, *Appl. Phys. Lett.* **84**, 750 (2004).
- ²⁹A. D. Rata, A. Herklotz, K. Nenkov, L. Schultz, and K. Dörr, *Phys. Rev. Lett.* **100**, 076401 (2008).
- ³⁰X. Zhao, J. Wang, Z. Peng, H. L. W. Chan, H. Luo, and C. L. Choy, *Phys. Status Solidi A* **198**, R1 (2003).
- ³¹A. Herklotz, J. D. Plümhof, A. Rastelli, O. G. Schmidt, L. Schultz, and K. Dörr, *J. Appl. Phys.* **108**, 094101 (2010).
- ³²C. H. Ahn, R. H. Hammond, T. H. Geballe, M. R. Beasley, J. M. Triscone, M. Decroux, O. Fischer, L. Antognazza, and K. Char, *Appl. Phys. Lett.* **70**, 206 (1997).
- ³³S. P. Singh, A. K. Singh, D. Pandey, and S. M. Yusuf, *Phys. Rev. B* **76**, 054102 (2007).